

EXAMINING ZINC OXIDE-CELLULOSE NANOPARTICLE COATINGS' CORROSION RESISTANCE ON MILD STEEL IN SODIUM CHLORIDE MEDIA

^{1,*}B.U. ANYANWU, ²S.O. OWOEYE, ¹O.O.OLAMIDE, ¹K.L. OLAITAN,
²F.O. DURODOLA, ¹O.R. ADETUNJI AND ¹A.D. ANIBABA

¹Mechanical Engineering Department, Federal University of Agriculture, Abeokuta,
Nigeria.

²Mechatronics Engineering Department, Federal University of Agriculture, Abeokuta,
Nigeria.

*Corresponding Author: anyanwubu@funaab.edu.ng

ABSTRACT

Chloride-induced corrosion of mild steel is a major challenge in construction, automobile, agro-processing, oil and gas industries. When chloride ions come in contact with mild steel surfaces, they penetrate the oxide layer and react with the metal, leading to the formation of corrosion products such as iron chloride that accelerates its degradation and consequent failure in service. Structurally enhanced metallic oxides and biopolymers have been reported to hinder the penetration and progression of these ions to the base metals, when deposited on them. This study's objective was to use electro-deposition to apply zinc oxide-cellulose ($x\text{ZnO}-x\text{C}_n$) nanoparticle coatings to mild steel (the substrate) in order to increase corrosion resistance in sodium chloride media. Weight loss technique was used to determine the corrosion rates of the deposited coatings (samples). Optical and scanning electron microscopy was used to determine the samples' morphology. The corrosion rate values of all the coatings were observed lower than the substrate's, which was 5.0025 mm/y. With the lowest corrosion rate value of 0.3127 mm/y, sample P8 (20gZnO-20gC_n) demonstrated a 93% coating protection efficiency on the substrate. Sample P1 (20gZnO-5gC_n) had the highest corrosion rate of 1.8954 mm/y and the highest protection efficiency of 62% among the coatings. The surface of the substrates showed fine, uniformly distributed grains according to the coating morphologies. The study demonstrated that in the sodium chloride media, ZnO-cellulose nanoparticle coatings could create protective barriers on the substrate.

Keywords: Chloride, deposition, particles, substrates, corrosion

INTRODUCTION

Corrosion is a natural process that occurs when metals are exposed to environments that promote chemical reactions. In the case of mild steel, the corrosion process is particularly significant in sodium chloride media. This form of corrosion, known as chlo-

ride-induced corrosion, is a major concern in various industries, such as construction, agro-processing, oil and gas, to mention, but a few.

Chloride-induced corrosion of mild steel in sodium chloride media occurs due to the

presence of chloride ions, which have a detrimental effect on the protective oxide layer of the steel (El-Sherik, 2016). When chloride ions come into contact with the mild steel surface, they penetrate the oxide layer and react with the metal, leading to the formation of corrosion products such as iron chloride. The corrosion process is influenced by various factors, like temperature, pH, and concentration of chloride ions. Higher temperatures accelerate the corrosion rate, while low pH levels and high chloride concentrations increase the aggressiveness of the environment (Patra, 2019). The presence of impurities and other corrosive substances can further enhance the corrosion process.

Several studies have been conducted to understand the mechanisms of chloride-induced corrosion of mild steel in sodium chloride media. According to Zhang (2015), the corrosion process involves an initial stage of pitting corrosion, where localized pits form on the steel surface. These pits then propagate, leading to the formation of larger corrosion sites. The presence of chloride ions accelerates the pit propagation rate, resulting in rapid corrosion of the steel. In addition to oxygen, the pH of the sodium chloride media can also impact the corrosion rate. Research by Patra (2019) noted that reduced pH and high acidic environmental conditions increase the aggressiveness of environment housing steel products and applications, thus, leading to higher corrosion rates. This is attributed to the increased availability of hydrogen ions, which enhance the dissolution of iron and the formation of corrosion products. The concentration of chloride ions in the media is another crucial factor affecting the corrosion of mild steel. Higher chloride concentrations create a more corrosive environ-

ment, as they increase the likelihood of chloride penetration into the oxide layer and subsequent reaction with the metal. Studies by El-Sherik, (2016) have demonstrated a direct correlation between chloride concentration and corrosion rate. Hence, corrosion / material engineers, continually seek to develop new techniques to improve the structural integrities of mild steel in domestic , industrial, automobile, marine and agro-allied processing applications, in chloride, alkaline or acidic media (Fayomi *et al.* 2021b; Anyanwu *et al.*, 2021b).

Several methods like heat treatment, electro-deposition coatings, cathodic protection etc. have been developed to improve the corrosion resistance properties of mild steel (Popoola and Fayomi, 2012; Anyanwu *et al.*, 2021a; Anyanwu *et al.*, 2021b). Although, some of these methods have provided improvements and enhancement in the overall properties, they are not cost effective; particularly as they require equipment with very high precision and further processing steps to produce high-grade steel components (Fayomi *et al.*, 2017).

The use of electro-deposition coatings in corrosion prevention is a relatively modern technology that involves less complex equipment. The method can prevent structural damage, while improving the corrosion resistance properties of mild steel, thus extending the materials life span, (Anyanwu *etal*, 2023; Odetola *etal*, 2016; Popoola and 2012). One electrochemical method used to alter surface structure is electro-deposition. It is regarded as a simple and affordable surface modification method for applying synthetic and organic coatings to metallic surfaces. An extensive variation of coating properties can be attained by selecting different parameters in electro-deposition

(Praveen and Venkatesh 2011). In a typical electro-deposition process, monolayer or multilayer (binary, ternary or quaternary) coatings are formed because of the electrochemical reactions occurring at the electrode/electrolyte interface and ions deposition from the electroplating bath. The coatings are deposited on the material (substrate) to improve the corrosion resistance properties, tribological properties, lubrication properties, electrical conductance properties, thermal resistance properties and magnetic properties etc. Metals, ceramics, polymers, cellulose, metal oxides, nitrides, etc. have all been reportedly employed in electro-deposition process (Odetola *et al.*, 2016; Anyanwu *et al* 2021a; Anyanwu *et al* 2022, Anyanwu *et al* 2023).

Electro-deposition surface modification can be done with two current types, the direct current (DC) and pulse current (PC). The difference between these two methods is that, while in the direct current application, the current is continuously applied to the system, where as in the pulse current, the electrical current is alternated between two different values (Fayomi *et al.*, 2021a; Odetola *et al.*, 2016). Although, the properties of the deposited coatings can be adversely affected by the pulsating parameters in the electro-deposition process, better elements dispersion and coating uniformities in terms of throw power and edge coverage has been reported with the direct current electro-deposition method (Odetola *et al.*, 2016, Fayomi and Popoola, 2015, Popoola *et al.*, 2016).

Metal oxide – biopolymer composite coatings have been used successfully in improving the surface and structural integrities of mild steel in recent times (Fayomi and Popoola 2015; Zhang 2015, Anyanwu *et al*

2021a, Anyanwu *et al* 2021b, Anyanwu *et al* 2022, Anyanwu *et al*, 2023). Current researches show that there are growing interests in the co-deposition of nanoparticles, made from oxides of metals, metals, cellulose, ceramics, nitrides etc. on metallic substrates, to enhance the mechanical, corrosion and thermal properties (Meulendijks *et al.* 2017; Anyanwu *et al.*, 2021a). Their inclusion offers self-lubrication properties with improved corrosion resistance properties on the substrate (mild steel). A good number of their nano-particulates are in existence and are in great demand for the generation of composite coatings on steel and other metals. The most abundant biopolymers currently in use are cellulose and they are inexpensive (Chakraborty *et al.*, 2005). They are also environmentally friendly and presently, there are few researches on their electro-deposition despite having good potentials. Their nano-particles have been co-deposited separately on mild steel, silver, Ag and Copper, Cu metals successfully (Anyanwu *et al* 2021a; Anyanwu *et al* 2021b; Meulendijks *et al.* 2017).

Kenaf (*hibiscus cannabinus* L.) is a biopolymer (nano-cellulose) that grows in nearly every kind of soil and needs little to no pesticides. Nigeria and the majority of the world's countries cultivate it extensively. It is highly rich in natural fibers and has excellent mechanical properties due to its 90% cellulose content (Anyanwu *et al.* 2019a; Anyanwu *et al.* 2019b; Jonoobi *et al.* 2009). It has proven effective in creating metal matrix composites with exceptional properties (Anyanwu *et al.* 2021a).

Therefore, the purpose of this study was to use direct current (DC) electro-deposition to apply zinc oxide-cellulose nanoparticle coatings ($x\text{ZnO-xCn}$) to mild steel (substrates) in order to improve corrosion resistance prop-

erties in sodium chloride media.

Materials and Methods

The study adopted methods in line with procedures outlined in highly rated journals and standard codes, some of which are found in Anyanwu *et al.* 2021a, Anyanwu *et al.* 2021b, Anyanwu *et al.* 2022 and Anyanwu *et al.* 2023. Mild steel, zinc bars, kenaf-derived nanocellulose fibers, zinc oxide nanoparticles, zinc chloride, glycine, and thiourea are the main substances used.

Bath contents and deposition

To remove any remaining contaminants from the samples and create mirror-like free scale flaws, the substrate (mild steel) was polished using emery papers up to 500 grits. It was thereafter divided into 50 mm x 20 mm x 2 mm pieces. After being degreased with trichloroethylene and rinsed with water, the samples were activated for ten seconds using a 10% HCl solution. Distilled

water and analytical-grade chemicals made up the bath's contents. Zinc oxide nanoparticles, ZnO (20 g/L), glycine (10 g/L), thiourea (10 g/L), zinc chloride, ZnCl (100 g/L), and nano-cellulose fibers (5 g/L to 20 g/L) were all present. Table 1 displays the voltage applied and the nanoparticle composition. The 99.9% zinc bar served as the anode, and the pretreated substrate served as the cathode. The anode-to-cathode distance and immersion depth were maintained at the same levels. To mix and enable the dissolution of every particle, the bath solution was heated and kept at 40 degrees Celsius. A mechanical stirrer was then used to continuously stir it up to 1000 rpm in order to achieve electrolyte uniformity. Set potentials of 0.3 and 0.5V, a pH of 5.5, different nanoparticle concentrations, and a constant current density of 2.0 A/cm² were all used during the 20-minute deposition process. Following the deposition process, the samples were rinsed for five seconds in distilled water before be-

Table 1 Nanoparticulates Composition

Experiment no.	Nanoparticles blend	Voltage (V)	Sample ID
1	20gZnO-5gC _n	0.3	P1
2	20gZnO-10gC _n	0.3	P2
3	20gZnO-15gC _n	0.3	P3
4	20gZnO-20gC _n	0.3	P4
5	20gZnO-5gC _n	0.5	P5
6	20gZnO-10gC _n	0.5	P6
7	20gZnO-15gC _n	0.5	P7
8	20gZnO-20gC _n	0.5	P8
Control	As received mild steel substrate	-	C

Corrosion rate behaviour of the developed composite coatings and substrate.

Using the weight loss technique, the corrosion behavior of the substrate and the created composite coatings was examined. This was carried out in a 3.5 weight percent NaCl medium at room temperature. A weighing balance was used to weigh the 1 cm x 1 cm coupons both before and after they were submerged in the corrosion medium for 720, 1440, 2160, and 2880 hours,

$$CR = \frac{8.76 \times 10^4 \Delta W}{\rho AT} \dots\dots\dots(1)$$

$$E (\%) = (1 - \frac{CR_c}{CR}) \times 100 \dots\dots\dots(2)$$

$$\theta = (1 - \frac{CR_c}{CR}) \dots\dots\dots(3)$$

Where CR = Corrosion rate (mm/year), W= Weight loss (g), ρ = Density of the sample (g/mm³), A = Exposed area (cm²),

T = Exposure time (hours), CR_c = corrosion rate when coating was employed and

CR = corrosion rate without the coatings

Characterization of the samples

The samples' microstructures were examined using an optical microscope that had a 400X magnification. Following the corrosion analysis, this was completed. Additionally, at a 1000X magnification, the surface and internal morphologies of the developed coatings and substrate were assessed using a TESCAN scanning electron microscope to assess grain refinements and uniformity.

respectively. After that, the coupons were taken out, cleaned with acetone and water, and dried. The weight differential was measured and noted. The corrosion rates, protection efficiencies, E (%) and degree of surface coverage (θ) of the samples were then determined using equations 1, 2, and 3 (Anyanwu *et al.* 2021a and 2023).

RESULTS AND DISCUSSION

Corrosion behaviour of the samples

As the samples' exposure time and concentration of nanoparticle blends in the media increased, it was found that the corrosion rate values for every sample decreased (Tables 2 and 3). The strength of the nanoparticle layer covering on the mild steel surface may have something to do with this. The layers tend to keep the chloride ions from coming into direct contact with the substrate's surface, which lessens the likelihood that corrosion products will form (Anyanwu *et al.*, 2021a; Anyanwu *et al.* 2022; Anyanwu *et al.* 2023; Fayomi *et al.* 2021a). Again, as the exposure time increased, the corrosion rate values, which are functions of the samples' corresponding mass loss, increased for all samples. As can be seen from

the table, every sample provided corrosion rate values that were lower than those of the "as received" sample C. More so, sample P8 had the lowest average corrosion rate value, measuring 0.3127 mm/y, according to the results. The sample provided a degree of surface coverage of 0.93 and a protection efficiency of 93% on the substrate

when compared to the "as received" sample, which had an average corrosion rate value of 5.0025 mm/y (Table 4). Sample P1 had the highest corrosion rate value of 1.8954 mm/y among the coating samples, with a degree of surface coverage of 0.62 and protection efficiency of 62% (Table 5).

Table 2 Corrosion data of the samples at 0.3V

Time	720 Hours		1440 Hours		2160 Hours		2880 Hours		Ave. C.R (mm/y)
Sample ID	ΔW (g)	C.R (mm/y)							
P1	0.1292	2.0013	0.2560	1.9842	0.3670	1.8940	0.4390	1.7021	1.8954
P2	0.1230	1.9010	0.2392	1.8516	0.3501	1.8104	0.4521	1.7502	1.8283
P3	0.0852	1.3121	0.1671	1.2921	0.2290	1.1824	0.2580	0.9981	1.1962
P4	0.0580	0.9014	0.1080	0.8341	0.1210	0.6243	0.1341	0.5210	0.7202
C	0.3950	6.1215	0.7731	5.9931	0.7891	4.0767	0.9855	3.8185	5.0025

Table 3 Corrosion data of the samples at 0.5V

Time	720 Hours		1440 Hours		2160 Hours		2880 Hours		Ave. C.R (mm/y)
Sample ID	ΔW (g)	C.R (mm/y)							
P5	0.0780	1.2012	0.1530	1.1861	0.1911	0.9879	0.2440	0.9467	1.0805
P6	0.0451	0.6921	0.0821	0.6341	0.1160	0.5981	0.1401	0.5421	0.6166
P7	0.0391	0.6101	0.0771	0.5979	0.1121	0.5802	0.1481	0.5726	0.5902
P8	0.0251	0.3941	0.0412	0.3210	0.0560	0.2896	0.0640	0.2461	0.3127
C	0.3950	6.1215	0.7731	5.9931	0.7891	4.0767	0.9855	3.8185	5.0025

Table 4 Protection efficiency and degree of surface coverage samples at 0.3V

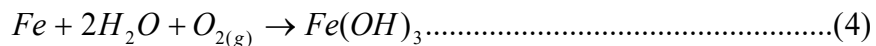
Samples	Degree of Surface Coverage (θ)	Protection Efficiency (%E)
P1	0.62	62
P2	0.64	64
P3	0.76	76
P4	0.86	86

Table 5 Protection efficiency and degree of surface coverage samples at 0.5V

Samples	Degree of Surface Coverage (θ)	Protection Efficiency (%E)
P5	0.78	78
P6	0.88	88
P7	0.88	88
P8	0.93	93

The mechanism of corrosion in this study involves the formation of corrosion products / rust (iron hydroxide), dissolution of iron ions, formation of ferrous chloride, acidification of the solution, and the generation of hydrogen gas (Fontana, 1986, Patra 2019). They are summarized on equations 4 – 9.

Formation of iron oxide:



In the presence of oxygen (O₂) and water (H₂O), iron (Fe) reacts to form iron hydroxide (Fe(OH)₃), which is commonly known as corrosion products /rust. This is then followed by the dissolution of iron ions:



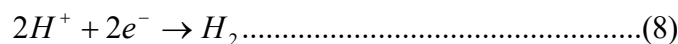
The iron hydroxide (Fe(OH)₃) formed in the previous step reacts with hydrogen ions (H⁺) to form iron ions (Fe³⁺) and water (H₂O). This is followed by the formation of ferrous chloride:



Iron (Fe) reacts with chloride ions (Cl⁻) to form ferrous chloride (FeCl₂), followed by the acidification of the solution:



Water (H₂O) dissociates into hydrogen ions (H⁺) and hydroxide ions (OH⁻), followed by the formation of hydrogen gas:



Hydrogen ions (H⁺) gain electrons (e⁻) to form hydrogen gas (H₂).

Overall reaction:



Ions move from the metal surface to the bulk of the solution when the samples come into contact with the corrosive media, which causes corrosion. However, the protective nanoparticle coatings on the substrate prevent this migration, which prevents the samples and the corrosive media from reacting further. The substrate sample's corrosion rates are considerably reduced as a result of this effect. When compared to coating samples deposited at 0.3V, those developed at a higher voltage (0.5V) demonstrated superior corrosion resistance characteristics. This is related to the fact that higher voltage tends to make electrons move more quickly, which guarantees faster and faster particulate deposition in the cathode substrate and, ultimately, uniform coating deposition (citation needed). The chemical affinities of the nanoparticles' conductance in the bath may also be linked to the coatings' efficacy. The coating deposits would not be uniform if the bath lost conductance, which would impact the sample's corrosion behavior (Odetola *et al.* 2016, An-

yanwu *et al.* 2021a, 2023, Fayomi *et al.* 2017).

Characterization of the samples

The SEM/EDS spectra of the mild steel sample (substrate) as received are displayed in Figure 1. It is evident that the steel's acceptable carbon content (0.26%) is met (Anyanwu *et al.*, 2021a). The corrosion study was conducted after the image and spectra were taken. Every coating had homogeneous and evenly spaced grains, no porosity, and good coating adherence (Figure 2). Additionally, they demonstrated strong throw power and edge protection, both of which support and improve the structural integrity and performance of coatings. Zinc (Zn), magnesium (Mg), carbon (C), and a trace amount of oxygen (O) and hydrogen (H) were present in the compositions of all the coating samples (Figure 3). The utilization of nanocellulose particles may have contributed to the carbon, oxygen, and hydrogen contents (Anyanwu *et al.* 2021a, 2021b, 2022, Noor and Al-Moubaraki, 2008).

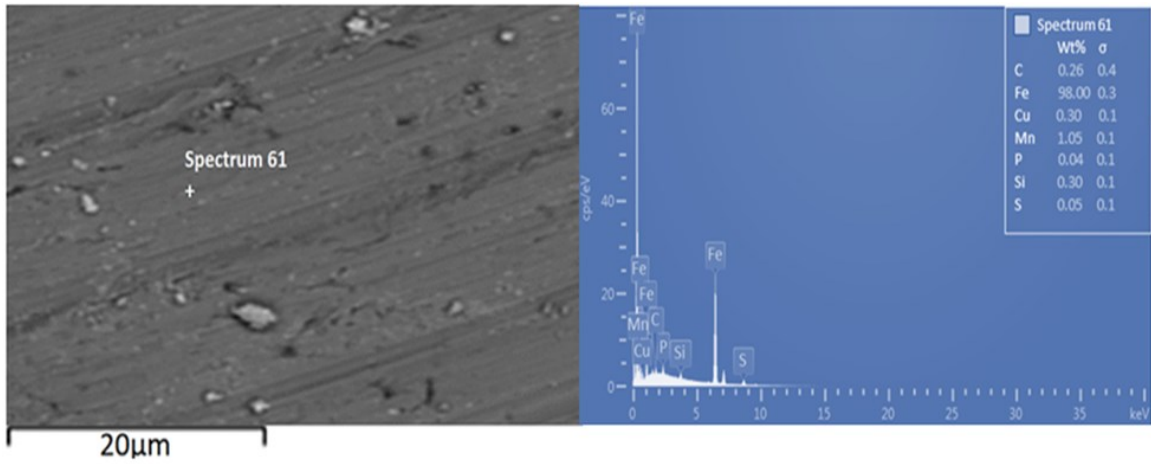


Figure 1: SEM / EDS Spectra of the as received mild steel (Sample C)

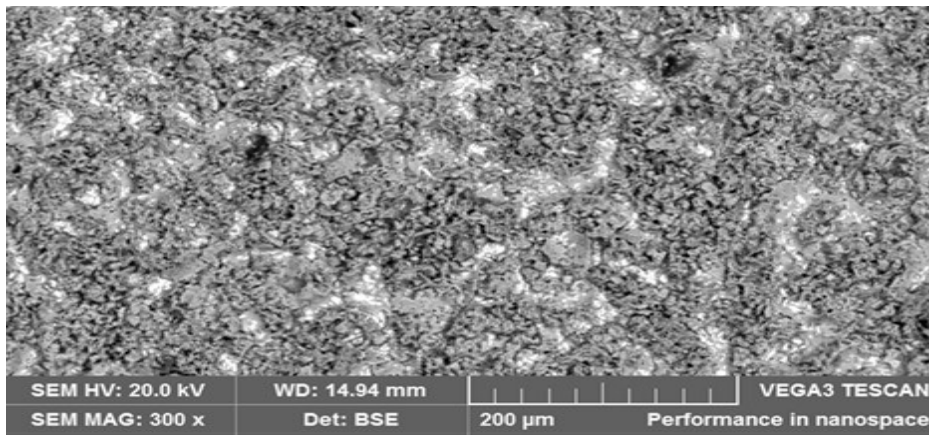


Figure 2: SEM imaging of the Coatings (Sample P8)



Figure 3: EDS Spectra of the Coatings (Sample P8)

Following the samples' exposure to the corrosive media, the optical microscopic images were taken. The images demonstrate how the attack from the corrosive media caused the "as received" sample to exhibit a significant corrosive effect. Its surface produces a greater number of corrosive products than the surfaces of the developed coatings (Figure 4). On the surfaces of the developed coatings, however, there were not

many pitting corrosion spots, particularly on sample P8. The sample's improved coating adherence, edge coverage, and coating throw power, as shown by the SEM spectra, may have something to do with this. According to studies, coatings with sufficient edge coverage, adherence, and throw power provide excellent performance while in use (Anyanwu et al., 2021a, 2023; Fayomi et al., 2017c, Popoola et al., 2016).

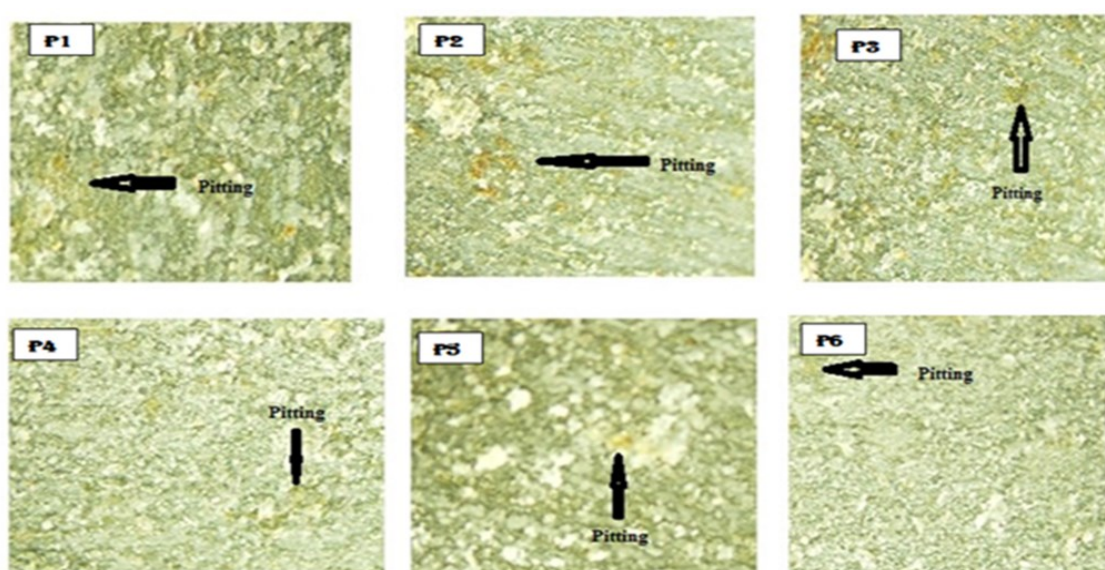


Figure 4: OPM images of all samples after exposure in the corrosive media

CONCLUSION

By using the electro-deposition method, the zinc oxide-cellulose nanoparticles ($x\text{-ZnO-xC}_n$) were successfully deposited on mild steel substrates. The sample coatings exhibited good throw power, edge coverage, uniformity, and coating adherence. This explained why their corrosion rate values were lower than those of the mild steel sample used in the investigation. With the lowest corrosion rate value of 0.3127 mm/y, Sample P8 (20gZnO-20gC_n) demonstrated a 93% protection efficiency on the mild steel. According to the study, the zinc oxide-

cellulose nanoparticle coatings prevented a subsequent reaction that would have intensified the mild steel sample's corrosion by preventing the migration of chloride ions to the substrate. This effect enhanced the sample's resistance to corrosion and dramatically decreased the rates of corrosion.

REFERENCES

Anyanwu B. U, Oluwole O. O, Fayomi O. S. I, Olorunnisola A. O, Popoola A.P.I, Kuye S.I, Wan Nik W. B. Oluwasegun K. M 2023. Assessing the impact of Zn-MgO-

- xC_n Ternary Coatings on A36 Low Carbon Steels for Oil and Gas Pipeline Applications, *Portugaliae Electrochimica Acta*, 41:301–313. doi.org/10.4152/pea.2023410404
- Anyanwu B.U; Oluwole O.O; Fayomi O.S.I; Olorunnisola A.O; Kuye S.I; Owoeye S.O., Olamide O.O** 2022. Polarization Corrosion Effects of Nanocellulose Reinforced Zinc-Magnesium Oxide Coatings on A36 Steel in Acidic Media, *International Journal of Basic Science and Technology* 8(3): 168-177.
- Anyanwu B.U, O.O. Oluwole, Fayomi O.S.I, Olorunnisola A.O, Popoola A. P. I and Kuye S.I** 2021a. Processing and development of corrosion resistance surface-active thin film nanocellulose composite coatings for mild steel protection, *Protection of Metals and Physical Chemistry of Surfaces*, 57(6): 1206–1213. DOI: 10.1134/S2070205121060034.
- Anyanwu B.U, Oluwole O.O, Fayomi O.S.I, Olorunnisola A.O, Popoola A.P.I and Kuye S.I** 2021b. Synthesis, corrosion and structural characterization of kenaf nanocellulose on Zn-ZnO-xC_n electrolytic coatings of mild steel for advanced applications, *Case Studies in Chemical and Environmental Engineering*, 3:1-5. doi.org/10.1016/j.cscee.2020.100017.
- Anyanwu B.U, Adebomi O. A, Fayomi O.S, Kuye S. I, Igba U.T and Oluwole O.O** 2019a. Effects of kenaf core and bast fibers as dispersing phases on low density fiberboards (engineered wood), *Journal of Physics: Conf. Series*, Vol. 1378, 022024. doi:10.1088/1742-6596/1378/2/022024.
- Anyanwu B.U, Olayinka G.O, Ezeokeke, D.T, Fayomi O.S and Oluwole O.O** 2019b. Effect of Kenaf Core Fibre (Hibiscus cannabinus) as one of the Dispersing Phases in Brake Pad Composite Production, *Journal of Physics: Conf. Series*, Vol. 1378, 042046. doi:10.1088/1742-6596/1378/4/042046.
- Chakraborty A, Sain M, and Kortschot M** 2005. Cellulose Microfibrils: A novel method of preparation using high shear refining and cryo crushing, *Holzforschung*, 59: 102-10.
- El-Sherik A. M** 2016. The effect of chloride ion concentration on the corrosion behavior of mild steel in alkaline medium, *Journal of Materials Science and Chemical Engineering*, 4(5), 1-9.
- Fayomi Ojo Sunday Isaac, Sode Ayodeji Adedamola, Anyanwu Benedict Uche, Nkiko Mojisola Olubunmi and Dauda Khadijah Tolulope** 2021a. Effect of Electrodeposition Mechanism and α -Si₃N₄/ZrBr₂ Doped Composite Particle on the Physicochemical and Structural Properties of Processed NiPZn Coatings on Mild Steel for Advance Application, *Key Engineering Materials*, 900(61-73). doi:10.4028/www.scientific.net/KEM.900.61
- Fayomi O.S.I, Sode A.A, Anyanwu B.U, Ayoola A.A, Nkiko M.O, Oluwasegun K.M, Alkhuele D.O., Ighravwe D.E** (2021b). Experimental studies and influence of process factor on zinc-nickel based coating on mild steel, *Advances in Materials and Processing Technologies* 8(2): 2193-2202. DOI: 10.1080/2374068X.2021.1896863
- Fayomi O.S.I, Joseph O.O and Popoola**

- A.P.I** (2017). Structural properties and micro-hardness performance of induced composite coatings filled with cocosnucifera-tin functionalized oxide, *Energy Proceedia*, 119: 910-915.
- Fayomi O.S.I and Popoola A.P.I (2015). Development of smart oxidation and corrosion resistance of multi-doped complex hybrid coatings on mild steel, *J. Alloys Compd.* 637: 382–392.
- Fontana M.G (1986). Corrosion Engineering, *McGrwa- Hill Publications*
- Jonoobi M. Harun J, Shakeri A, Misra M and Oksman K (2009). Chemical composition, crystallinity and thermal degradation of bleached and unbleached kenaf bast (*Hibiscus cannabinus*) pulp and nanofibers, *BioResources* 4 (2):626– 639.
- Meulendijks N, Burghoorn M, Mourad M, Mann D, Keul H, Bex G, Veldhoven E, Verheijen M., Buskens P** 2017. Electrically conductive coatings consisting of Ag-decorated cellulose nanocrystals, *Cellulose*, 24: 2191–2204.
- Noor E.A and Al-Moubaraki A.H** 2008. Corrosion Behavior of Mild Steel in Hydrochloric Acid Solutions, *International Journal of Electrochemical Science*, 3: 806-818.
- Odetola P, Popoola P, Popoola O., Delport D** 2016. Parametric Variables in Electro-deposition of Composite Coatings, *INTECH Open Science /Open Minds* <http://dx.doi.org/10.5772/62010>.
- Patra P (2019). Influence of pH on the corrosion behavior of mild steel in NaCl solution, *Materials Today: Proceedings*, 15, 225-231.
- Popoola A.P.I, Aigbodion V.S, and Fayomi O.S.I (2016). Surface characterization, mechanical properties and corrosion behaviour of ternary based Zn-ZnO-SiO₂ composite coating of mild steel, *Journal of Alloys and Compounds*, 654: 561-566.
- Popoola A.P.I and Fayomi O.S.I (2012). Performance evaluation of zinc deposited mild steel in chloride medium, *International Journal of Electrochemical Science*, 6: 3254-3326.
- Praveen B.M and Venkatesh T.V (2011). Electro-deposition and corrosion resistance properties of Zn-Ni/TiO₂ nano composite coating, *International Journal of Electrochemical Science*, 261: 407-792.
- Zhang F (2015). Effect of chloride ion concentration on the corrosion behavior of mild steel in simulated concrete pore solutions,

(Manuscript received:23rd July, 2024; accepted: 20th December, 2024).